

## Simulations of atomic processes at semiconductor surfaces: General method and chemisorption on GaAs(110)

Madhu Menon and Roland E. Allen

Center for Theoretical Physics, Department of Physics, Texas A&M University, College Station, Texas 77843-4242

(Received 20 August 1987; revised manuscript received 21 March 1988)

Recently we introduced a technique for realistic simulations of atomic motion in systems with covalent or metallic bonding. The technique involves the Hellmann-Feynman theorem, novel Green's-function methods, and integration in the complex energy plane. In principle, it is exact, so that one can use a self-consistent Hamiltonian and even include many-body effects. Here we provide some refinements of this general technique which simplify its use in practical calculations. We also describe an approximate version that employs a tight-binding Hamiltonian and repulsive potential. Representative simulations are shown for atoms of groups I-VII chemisorbing on the (110) surface of GaAs.

### I. INTRODUCTION

Recently we introduced a technique for realistic simulations of atomic motion in systems with covalent or metallic bonding.<sup>1-7</sup> The essential idea is to compute the atomic forces directly from the electronic structure, via the Hellmann-Feynman theorem. This problem is reduced to manageable proportions with the use of novel Green's-function methods and integration in the complex energy plane.<sup>3</sup>

In the present paper, we (1) provide some refinements of the general technique, (2) describe an approximate version that employs a tight-binding Hamiltonian<sup>8-14</sup> and repulsive potential,<sup>15</sup> and (3) demonstrate that the method works by showing results for time-dependent chemisorption on GaAs(110).

### II. METHOD

#### A. General ideas

The force  $F_x$  associated with some atomic coordinate  $x$  is given by

$$F_x = -\frac{\partial U}{\partial x}, \quad (2.1)$$

where  $U$  is the total energy of the system. If  $F_x$  can be calculated, numerical solution of the equation of motion

$$m \frac{d^2 x}{dt^2} = F_x \quad (2.2)$$

is straightforward, and one can perform molecular dynamics computer simulations.<sup>16-30</sup>

In the present approach,  $F_x$  is calculated from the electronic structure,<sup>1-7,24,31</sup> rather than classical  $n$ -body potentials.<sup>32-38</sup> Let the electrons be divided into valence electrons, whose states will be regarded as adiabatically changing in response to the motion of the nuclei, and core electrons, whose states will be regarded as rigidly

following the nuclei. There are three contributions to the total energy  $U$ :

$$U = U_{el} - U_{ee} + U_{ions}. \quad (2.3)$$

Our approximate treatment of (2.3) will be essentially the same as that of Chadi.<sup>12</sup> In representing the last two terms ( $U_{ions} - U_{ee}$ ) we will use a repulsive potential  $\phi(r)$ , rather than Chadi's quadratic expansion ( $U_1 \epsilon + U_2 \epsilon^2$ ) in the bond-length change  $\epsilon$ . There is no difference, however, in the basic philosophy.

Since the present technique employs Green's functions, one could include many-body effects in the treatment of  $U$ . In this paper, however, we will assume a one-electron picture throughout. Then  $U_{el}$  is the sum of the energies  $\epsilon_k$  of the occupied one-electron states:

$$U_{el} = \sum_k^{\text{occupied}} \epsilon_k. \quad (2.4)$$

Also,  $U_{ee}$  is the energy associated with the electron-electron Coulomb repulsion, which is doubly counted in (2.4), and  $U_{ions}$  is the ion-ion Coulomb repulsion, with an ion defined to be the atomic nucleus plus core electrons.

One can regard the interaction between two atoms as consisting of (1) an attractive bonding interaction involving the one-electron energies  $\epsilon_k$  and (2) a repulsive interaction representing a combination of effects, including the Pauli exclusion principle and the direct ion-ion repulsion. In the calculations of the present paper, we will therefore model (2.3) by

$$U = U_{el} + U_{rep} \quad (2.5)$$

with  $U_{rep}$  given by a repulsive pair potential  $\phi(r)$ :

$$U_{rep} = \sum_i \sum_{j (> i)} \phi(r_{ij}). \quad (2.6)$$

Here  $r_{ij}$  is the separation of atoms  $i$  and  $j$ . We will also calculate the electronic energies  $\epsilon_k$  using a semi empirical tight-binding Hamiltonian,<sup>10</sup> with the intra-atomic matrix elements  $H_{ii}$  regarded as atomic energies, and the in-

teratomic elements  $H_{ij}$  representing an overlap of the electronic wave functions. The  $H_{ii}$  are taken to be constant, and the  $H_{ij}$  are taken to decrease exponentially with the interatomic separation  $r$ . To be precise, let  $H_{ij}(\alpha, \beta)$  be the Hamiltonian matrix element coupling orbital  $\alpha$  on atom  $i$  to orbital  $\beta$  on atom  $j$ . This element is given by the direction cosines  $l = \Delta x / r$ , etc., and by primitive tight-binding matrix elements  $V_{ss\sigma}$ , etc. (See p. 481 of Ref. 10, or the original paper of Slater and Kostler.<sup>8</sup>) For example, the matrix element  $H_{ij}(p_x, p_y)$  coupling a  $p_x$  orbital to a  $p_y$  orbital is given by  $V_{pp\sigma}(r)$  and  $V_{pp\pi}(r)$ . We take each primitive element  $V(r)$  to decrease exponentially with  $r$ :

$$V(r) = V(r_0) \exp[-\alpha(r - r_0)]. \quad (2.7a)$$

For the parameters employed in the present work— $V_{ss\sigma}$ ,  $V_{sp\sigma}$ ,  $V_{pp\sigma}$ , and  $V_{pp\pi}$ —we choose  $\alpha = 2/r_0$ . As mentioned above (2.18), one can fit  $\alpha$  to the bond-stretching force constant of the solid; however, the argument given there indicates that the present simple choice is not a bad approximation.

We fit each  $V(r_0)$  ( $V_{ss\sigma}$  etc.) to its value in Ref. 10 at some fixed distance  $r_0$  which represents a typical bond length. To be specific, we take  $r_0$  to be the bondlength of the solid (2.45 Å for GaAs and 2.54 Å for InP). Since the present work involves only  $s$  and  $p$  electrons, for which the scaling of Ref. 10 is  $V_H(r) = V(r_0)(r_0/r)^2$ , we have  $[dV(r)/dr]_{r=r_0} = -\alpha V(r_0)$  and  $[dV_H(r)/dr]_{r=r_0} = (-2/r_0)V_H(r_0)$ . Our choice  $\alpha = 2/r_0$  thus matches the present logarithmic derivatives at  $r = r_0$  to those of Ref. 10.

The repulsive potential is also assumed to decrease exponentially with  $r$ ,

$$\phi(r) = \phi_0 \exp[-\beta(r - d)], \quad (2.7b)$$

but in this case we take  $d$  to equal the sum of the covalent radii of the two interacting atoms. I.e., we take the range of the repulsive interaction to scale with the size of the atom. If the attractive (electronic) interaction is to dominate at large distances, and the repulsive interaction at small distances,  $\beta$  should be larger than  $\alpha$ . One could try to optimize  $\beta$ , but we simply choose  $\beta = 2\alpha$ .

This leaves the parameter  $\phi_0$ , which is determined by the requirement that the total energy of (2.4)–(2.6) for the bulk solid be a minimum at  $r = r_0$ , where  $r_0$  is the experimental bondlength. Specifically, we fit  $\phi(r)$  to the repulsive potential of Harrison and co-workers<sup>15</sup> and Sankey,<sup>5</sup>  $\phi_H(r) = C/r^4$ , at  $r = r_0$ . Notice that  $[d\phi(r)/dr]_{r=r_0} = -\beta\phi(r_0)$  and  $[d\phi_H(r)/dr]_{r=r_0} = (-4/r_0)\phi_H(r_0)$ , so our choice  $\beta = 4/r_0$  matches the present logarithmic derivative of  $\phi$  at  $r = r_0$  to that of Ref. 15.

Finally, since nearest-neighbor interactions are more chemically meaningful than distant interactions, we truncate both  $V(r)$  and  $\phi(r)$ ; specifically, we take  $V(r) = 0$  and  $\phi(r) = 0$  for  $r > R_c = 1.25r_0$ . One could smooth out the delta-function singularity in the radial force at  $R_c$ , but this would make only a small difference in the present simulations. One could also, of course, choose a less conservative value for  $R_c$ .

Notice that only three parameters distinguish a chemical species—the  $s$  and  $p$  atomic energies,  $\epsilon_s$  and  $\epsilon_p$ —which determine the atom's electronegativity—and the covalent radius  $r_c$ —which determines its size. We can represent  $\epsilon_s$  and  $\epsilon_p$  approximately by an average or “hybrid” energy

$$\bar{\epsilon} = (\epsilon_s + 3\epsilon_p) / 4. \quad (2.8)$$

All electronic states below the Fermi energy  $\epsilon_F$  of the solid are assumed to be occupied, and all states above  $\epsilon_F$  to be empty. Our use of a cutoff  $R_c$  makes this assumption physically reasonable: If an atom impinging on the surface is outside the range of interaction, there are no forces and its occupancy is irrelevant. As soon as it is within the interaction range, it is interacting rather strongly, forming bonding and antibonding states with the solid, and its occupancy should be approximately correct.

Calculation of the repulsive forces associated with  $U_{\text{rep}}$  is straightforward, so the remainder of this section will be dedicated to a discussion of the electronic forces associated with  $U_{\text{el}}$ .

## B. Simple examples

Before turning to a detailed description of the present technique, let us consider two simple examples—a pair of atoms with one orbital per atom, and a cluster of  $n_{\text{cl}}$  atoms with a general tight-binding Hamiltonian.

In each of these examples, the Schrödinger equation is

$$H\psi_i^{\text{cl}} = \epsilon_i^{\text{cl}}\psi_i^{\text{cl}}, \quad (2.9)$$

with  $H$  an  $n \times n$  matrix if there are  $n$  orbitals. For the pair of atoms, we have  $n = 2$  and

$$H = \begin{pmatrix} \epsilon_1 & V \\ V & \epsilon_2 \end{pmatrix}, \quad (2.10)$$

where  $\epsilon_1$  and  $\epsilon_2$  are the atomic energies of the two atoms and  $V$  is the interatomic matrix element. The bonding and antibonding states have energies

$$\epsilon_{\pm} = \frac{1}{2}(\epsilon_1 + \epsilon_2) \pm \frac{1}{2}[(\epsilon_1 - \epsilon_2)^2 + 4V(r)^2]^{1/2}. \quad (2.11)$$

Since the bonding state is doubly occupied and the antibonding state unoccupied, the total energy of (2.5) is

$$U(r) = 2\epsilon_- + \phi(r). \quad (2.12)$$

As  $r$  decreases,  $|V(r)|$  increases, so  $\epsilon_-$  decreases and the electronic force is attractive. The total force  $F$  is given by the scaling rules (2.7):

$$F(r) = -\frac{dU(r)}{dr} \quad (2.13)$$

$$= -2\alpha \left[ 1 + \left[ \frac{\epsilon_1 - \epsilon_2}{2V(r)} \right]^2 \right]^{-1/2} |V(r)| + \beta\phi(r). \quad (2.14)$$

For identical atoms this becomes

$$F(r) = -2\alpha |V(r)| + \beta\phi(r), \quad (2.15)$$

so the strength of the electronic force is determined by the interatomic matrix element  $V(r)$  and its dependence on the separation of the atoms  $r$ .

The equilibrium separation is given by  $2\alpha |V(r)| = \beta\phi(r)$ , or

$$r = \{\ln[2\alpha |V(r_0)| / \beta\phi_0] + (\alpha r_0 - \beta d)\} / (\alpha - \beta). \quad (2.16)$$

If we choose  $\beta = 2\alpha$  and  $\phi_0 = |V(r_0)|$ , (2.16) becomes

$$r = 2d - r_0. \quad (2.17)$$

We are still free to choose  $r_0 = d_0$ , where  $d_0/2$  is the covalent radius for some particular species of atom. Then the equilibrium separation of (2.17) will be exactly equal to the correct value  $d_0$  for this one species. This choice of  $r_0$ , and thus  $\phi_0$ , is analogous to our choice in the real problem, namely, we define  $r_0$  to be the experimental bond length within the solid, and we choose  $\phi_0$  such that the model correctly reproduces this bond length.

Although we have simply taken  $\alpha = 2/r_0$  in the present paper, one could determine  $\alpha$  by fitting the bond-stretching force constant  $K$  in the solid. This idea is again illustrated by the above pair of atoms with covalent radius  $d_0/2$ : Eq. (2.15) gives

$$\frac{dF(r)}{dr} = 2\alpha^2 |V(r)| - \beta^2\phi(r) \quad (2.18)$$

so

$$\left[ \frac{dF(r)}{dr} \right]_{r=r_0} = -2\alpha^2 |V(r_0)| \quad (2.19)$$

or

$$K = 2\alpha^2 |V(r_0)| \quad (2.20)$$

for the above choice of  $\beta$ ,  $\phi_0$ , and  $r_0$ . If  $|V(r_0)|$  is determined by fitting the gap between bonding and anti-bonding states,

$$\epsilon_{\text{gap}}(r_0) = \epsilon_+ - \epsilon_- = 2 |V(r_0)|, \quad (2.21)$$

then  $\alpha$  is determined by (2.20). For a typical semiconductor, the most important matrix element  $V_{pp\sigma}$  (determined by fitting the bulk band structure) is  $\approx 4$  eV, and the force constant  $K$  is  $\approx 40$  eV/ $r_0^2$ ,<sup>10</sup> so (2.20) gives  $\alpha \approx \sqrt{5}/r_0$ . This indicates that our choice  $\alpha = 2/r_0$  is not a bad approximation. We also note that the choice  $\phi_0 = |V(r_0)|$  for the pair of atoms is in approximate agreement with the values of  $\phi_0$  obtained for the real solids, i.e.,  $\phi_0 \approx V_{pp\sigma}$ .<sup>5,15</sup>

Now let us consider a general cluster of atoms with  $s$ ,  $p$  and  $d$  electrons. The tight-binding Hamiltonian matrix for the cluster is easily constructed, using the atomic positions and the primitive tight-binding matrix elements  $V_{ss\sigma}$ ,  $V_{sp\sigma}$ ,  $V_{pp\sigma}$ ,  $V_{pp\pi}$ , etc.<sup>10</sup> Numerical solution of (2.9) gives the  $n$  eigenvalues  $\epsilon_i^{\text{cl}}$  and eigenvectors  $\psi_i^{\text{cl}}$ . The electronic force associated with a given atomic coordinate  $x$  can then be computed from the Hellmann-Feynman theorem:

$$F_x^{\text{el}} = - \frac{\partial U_{\text{el}}}{\partial x} \quad (2.22)$$

$$= - \sum_i \frac{\partial \epsilon_i^{\text{cl}}}{\partial x} \Theta(\epsilon_F - \epsilon_i^{\text{cl}}), \quad (2.23)$$

$$\frac{\partial \epsilon_i^{\text{cl}}}{\partial x} = \psi_i^{\text{cl}\dagger} \frac{\partial H}{\partial x} \psi_i^{\text{cl}}. \quad (2.24)$$

We remark that the term ‘‘Hellmann-Feynman theorem’’ as used here has a meaning somewhat different from the conventional meaning,<sup>39</sup> involving wave functions  $\Psi(r_1, r_2, \dots, r_N)$  in real space. In that context, the wave functions must be calculated with considerable accuracy if one is to obtain reliable atomic forces. Our Hellmann-Feynman theorem (2.24) or (2.31), on the other hand, gives the atomic forces *exactly* within the present model of the electronic structure. Since this model has been demonstrated to give reliable total energies and forces in, e.g., calculations of surface relaxation,<sup>5,12-14</sup> the forces calculated here should also be reliable. This is borne out by the results presented in the next section.

Using the above ideas, one can perform simulations of atomic motion in small clusters of atoms. At an early stage in the present program, we in fact carried out such simulations for one atom chemisorbing on a group of four additional atoms. These simulations were found to be very helpful as initial tests, since the mathematics is simple and the results relatively easy to interpret.

An isolated cluster of atoms, however, is only a crude approximation to a real solid surface. In the next subsection, therefore, we describe a method for treating a semi-infinite material. The central idea is to replace the Hamiltonian  $H$ , for an isolated cluster of  $n_{\text{cl}}$  atoms, by a ‘‘subspace Hamiltonian’’  $H_{\text{sub}}(\epsilon)$ , for a subspace of  $n_{\text{cl}}$  atoms within a semi-infinite (or infinite) system.

In the present approach, we allow a set of  $n_m$  atoms to move. The remaining atoms are taken to be motionless, but their effect on the electronic structure is included exactly, using Green’s-function methods. Since the motion of an atom alters its interaction with neighboring atoms, these neighbors must also be included in the perturbation subspace represented by  $H_{\text{sub}}$ . I.e., we have  $n_{\text{cl}} > n_m$ , where  $n_{\text{cl}}$  is the number of atoms in the perturbation subspace and  $n_m$  is the number in the ‘‘movement subspace.’’ We mention that one can include the motion of the atoms outside the movement subspace approximately—e.g., in the harmonic approximation (using the phonon Green’s function<sup>3,6,40</sup>) or in some stochastic approximation.<sup>41</sup> In the present paper, however, we treat these atoms as fixed at their equilibrium positions—with the surface relaxation<sup>42,43</sup> included—so that they influence the simulation only through their repulsive potentials and their effect on the electronic structure.

### C. Subspace Hamiltonian

Let  $\underline{H}$  be the Hamiltonian matrix of a system represented by  $N$  electronic orbitals (with  $N \rightarrow \infty$  in the problems of interest here). We suppose that  $\underline{H}$  differs

from an unperturbed Hamiltonian  $\underline{H}_0$  only in some  $n \times n$  block:

$$\underline{H} = \underline{H}_0 + \underline{V}, \quad (2.25)$$

$$\underline{V} = \begin{pmatrix} V^{11} & 0 \\ 0 & 0 \end{pmatrix}. \quad (2.26)$$

$\underline{H}$  and the Green's function  $\underline{G}$  are partitioned in the same way as  $\underline{V}$ ,<sup>3</sup>

$$\underline{H} = \begin{pmatrix} H^{11} & H^{12} \\ H^{21} & H^{22} \end{pmatrix}, \quad (2.27)$$

$$\underline{G} = \begin{pmatrix} G^{11} & G^{12} \\ G^{21} & G^{22} \end{pmatrix}, \quad (2.28)$$

and for notational convenience one defines  $V = V^{11}$ ,  $H = H^{11}$ , and  $G = G^{11}$ .

Let  $G_0$  be the unperturbed Green's function corresponding to  $H_0$ , and  $G_0 = G_0^{11}$ . We define the subspace Hamiltonian<sup>3</sup> by

$$\varepsilon - H_{\text{sub}}(\varepsilon) = G_0^{-1} - V. \quad (2.29)$$

In general  $H_{\text{sub}}$  is non-Hermitian, with right and left eigenvectors  $\psi_i$  and  $\bar{\psi}_i$ :

$$H_{\text{sub}}(\varepsilon)\psi_i(\varepsilon) = \varepsilon_i(\varepsilon)\psi_i(\varepsilon), \quad (2.30a)$$

$$H_{\text{sub}}^\dagger(\varepsilon)\bar{\psi}_i(\varepsilon) = \varepsilon_i^*(\varepsilon)\bar{\psi}_i(\varepsilon). \quad (2.30b)$$

The derivatives of the eigenvalues  $\varepsilon_i$  with respect to the atomic coordinates  $x$  are given by the Hellmann-Feynman theorem:<sup>3</sup>

$$\frac{\partial \varepsilon_i(\varepsilon)}{\partial x} = \bar{\psi}_i^\dagger(\varepsilon) \frac{\partial V}{\partial x} \psi_i(\varepsilon). \quad (2.31)$$

Notice that the calculation of

$$V = H - H_0, \quad (2.32)$$

with  $H_0 = H_0^{11}$ , is just as straightforward as calculation of the cluster Hamiltonian  $H$  of the preceding subsection. In fact,  $H$  is the Hamiltonian of the isolated cluster of  $n_{\text{cl}}$  atoms, and  $H_0$  is the special case of  $H$  when the atoms are at their initial, unperturbed positions. Notice also that  $\partial V / \partial x = \partial H / \partial x$  involves only the interatomic matrix elements, and is calculated from the scaling rule (2.7a).

The unperturbed Green's function  $G_0(\varepsilon)$  is relatively easy to calculate with the present technique because it is needed only at complex energies  $\varepsilon$ . One can therefore use the "naive" spectral representation of the Green's function, with no  $+i\delta$  in the denominator.

First consider the bulk Green's function  $G_b$ , which has the spectral representation

$$G_b(\mathbf{x}, \mathbf{x}'; \varepsilon) = \sum_{\mathbf{k}, s} \frac{u(\mathbf{x}; \mathbf{k}, s) u^\dagger(\mathbf{x}'; \mathbf{k}, s) e^{i\mathbf{k} \cdot (\mathbf{x} - \mathbf{x}')}}{\varepsilon - \varepsilon(\mathbf{k}, s)}, \quad (2.33)$$

where  $\mathbf{x}$  represents an atomic position. The electronic energies  $\varepsilon(\mathbf{k}, s)$  and the periodic part of the Bloch function,

$u(\mathbf{x}; \mathbf{k}, s)$ , are determined by the standard bulk eigenvalue equation

$$H_b(\mathbf{k})u(\mathbf{k}, s) = \varepsilon(\mathbf{k}, s)u(\mathbf{k}, s), \quad (2.34)$$

where  $\mathbf{k}$  is the wave vector and  $s$  the band index.

The unperturbed surface Green's function at a fixed planar wave vector  $\bar{k} = (k_1, k_2)$  can be obtained from a one-electron Dyson equation having the form

$$\bar{G}_0(\bar{k}, \varepsilon) = \bar{G}_b(\bar{k}, \varepsilon) + \bar{G}_b(\bar{k}, \varepsilon) \bar{V}_s(\bar{k}) \bar{G}_0(\bar{k}, \varepsilon). \quad (2.35)$$

We have used bars to indicate that these matrices are associated with atoms near the surface plane. It is just as straightforward to construct the surface perturbation matrix  $\bar{V}_s$  (in a tight-binding model) as it is to construct the  $V$  of (2.32) or the cluster Hamiltonian  $H$  of the preceding subsection. It is also straightforward to construct  $\bar{G}_b$  using (2.33).

After (2.35) has been solved numerically, one obtains  $G_0$  from

$$G_0(\mathbf{x}, \mathbf{x}'; \varepsilon) = \int d\bar{k} \bar{G}_0(\mathbf{x}, \mathbf{x}'; \bar{k}, \varepsilon) e^{i\bar{k} \cdot (\bar{x} - \bar{x}')}, \quad (2.36)$$

where  $\bar{x} = (x_1, x_2)$  is the planar coordinate, so that  $\mathbf{x} = (\bar{x}, x_3)$ . The integral of (2.36) is approximated by a summation over special points.<sup>44-46</sup> As  $|\bar{x} - \bar{x}'|$  increases in (2.36), we find that larger sets of special points are required for an accurate calculation of  $G_0$ . For example, 16 special points are required in the (110) surface Brillouin zone for a subspace with 4 surface and subsurface atoms, but 36 are required with 8 atoms. This trend is reasonable because there are more rapid oscillations with respect to  $\bar{k}$  in the integrand of (2.36) as  $|\bar{x} - \bar{x}'|$  increases, requiring a denser set of sample wave vectors. It is these oscillations, and the resulting destructive interference within the integral of (2.36), that cause  $G_0(\mathbf{x}, \mathbf{x}')$  to decrease to zero as  $|\bar{x} - \bar{x}'| \rightarrow \infty$ .

Even for very large  $\Delta\bar{x} \equiv \bar{x} - \bar{x}'$ , however, one can accurately evaluate (2.36) with only a few special points, if the rapidly varying function  $\exp(i\bar{k} \cdot \Delta\bar{x})$  is isolated from the slowly varying function  $\bar{G}_0(\bar{k})$ : Let  $A$  be the area of the surface Brillouin zone represented by the special point  $\bar{k}_0$ . The contribution of  $\bar{k}_0$  to (2.36) is then

$$\int_A d\bar{k} \bar{G}_0(\bar{k}) e^{i\bar{k} \cdot \Delta\bar{x}} \approx \bar{G}_0(\bar{k}_0) \int_A d\bar{k} e^{i\bar{k} \cdot \Delta\bar{x}}. \quad (2.37)$$

In the present calculations,  $A$  is rectangular, with width  $\Delta k_x$  and height  $\Delta k_y$ , so

$$\int_A d\bar{k} e^{i\bar{k} \cdot \Delta\bar{x}} = \frac{\sin(\frac{1}{2}\Delta k_x \Delta x)}{\frac{1}{2}\Delta x} \frac{\sin(\frac{1}{2}\Delta k_y \Delta y)}{\frac{1}{2}\Delta y} e^{i\bar{k}_0 \cdot \Delta\bar{x}}. \quad (2.38)$$

For small  $\Delta x$  and  $\Delta y$ , the factor multiplying  $\exp(i\bar{k}_0 \cdot \Delta\bar{x})$  is  $\Delta k_x \Delta k_y$ , but as  $\Delta x$  and  $\Delta y$  increase, this factor decreases because of the destructive interference within  $A$ .

#### D. Electronic force

In Ref. 3 it was proved that

$$H_{\text{sub}}(\epsilon) \rightarrow H \text{ as } |\epsilon| \rightarrow \infty, \quad (2.39a)$$

so

$$\epsilon_i(\epsilon) \rightarrow \epsilon_i^{\text{cl}} \text{ and } \psi_i(\epsilon) \rightarrow \psi_i^{\text{cl}}. \quad (2.39b)$$

It is also shown that the segment along the real axis between  $\epsilon_c$  and  $\epsilon_F$ , with  $\epsilon_c \rightarrow -\infty$ , can be deformed into the contour  $C_1$  plus  $C_2$  of Fig. 1. Here  $\epsilon_F$  is the Fermi energy, which lies within the band gap of the semiconductor. (To be specific, we choose it to lie at midgap, as for an intrinsic semiconductor.) We can make the replacement indicated by (2.39) along  $C_1$ , and also along the upper part of  $C_2$  from  $\epsilon_F + i\infty$  down to  $\epsilon_F + i\epsilon_{\text{max}}$ , where  $\epsilon_{\text{max}}$  is some energy that is large in comparison to  $|\epsilon_F - \epsilon_i^{\text{cl}}|$  for all of the  $\epsilon_i^{\text{cl}}$ . Then (7.4) of Ref. 3 implies that

$$F_x^{\text{el}} = F_1 + F_2 + F'_2, \quad (2.40)$$

where

$$F_1 = \frac{1}{\pi} \text{Im} \left[ \sum_i \frac{\partial \epsilon_i^{\text{cl}}}{\partial x} \ln \left[ \frac{\epsilon_a - \epsilon_i^{\text{cl}}}{\epsilon_c - \epsilon_i^{\text{cl}}} \right] \right], \quad (2.41)$$

$$F_2 = \sum_j F_j, \quad (2.42a)$$

$$F_j \approx \frac{1}{\pi} \text{Im} \left[ \sum_i \frac{\partial \epsilon_i(\epsilon_0^j)}{\partial x} \ln \left[ \frac{\epsilon_a^j - \epsilon_i(\epsilon_0^j)}{\epsilon_c^j - \epsilon_i(\epsilon_0^j)} \right] \right], \quad (2.42b)$$

$$F'_2 \approx \frac{1}{\pi} \text{Im} \left[ \sum_i \frac{\partial \epsilon_i^{\text{cl}}}{\partial x} \ln \left[ \frac{(\epsilon_F + i\epsilon_{\text{max}}) - \epsilon_i^{\text{cl}}}{\epsilon_a - \epsilon_i^{\text{cl}}} \right] \right]. \quad (2.43)$$

In (2.41) and (2.43),  $\epsilon_c = \epsilon_F - R$  and  $\epsilon_a = \epsilon_F + iR$  are the lower and upper endpoints of  $C_1$ , as depicted in Fig. 1. In (2.42b),  $\epsilon_0$  is a sample energy representing the segment of  $C_2$  between the upper point  $\epsilon_c^j$  and the lower point  $\epsilon_a^j$ . In order for (2.42b) to be a good approximation, the  $\epsilon_0^j$  should be more densely spaced as the real axis is approached, since  $\epsilon_i(\epsilon)$  and  $\psi_i(\epsilon)$  begin to deviate significantly from  $\epsilon_i^{\text{cl}}$  and  $\psi_i^{\text{cl}}$  as  $\text{Im}\epsilon \rightarrow 0$  along  $C_2$ . We

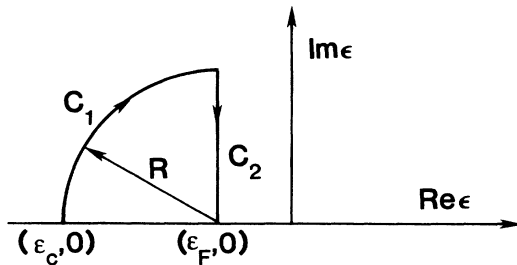


FIG. 1. Complex energy plane. Integration over the rapidly varying structure between  $\epsilon_c$  (an energy below the relevant electronic energy bands) and  $\epsilon_F$  (the Fermi energy of the solid) would require a very large number of sample energies for an accurate calculation. We replace this interval by a finite segment of  $C_2$  between  $\epsilon_F + i\epsilon_{\text{max}}$  and  $\epsilon_F$ . Since the eigenvalues of the subspace Hamiltonian are slowly varying functions of  $\epsilon$  for  $\epsilon$  complex, only a few sample energies are required.

find that an optimum choice of five sample energies  $\epsilon_0^j$  gives  $\sim 5\%$  accuracy in the calculated electronic force.

Let  $\Delta\epsilon \equiv \epsilon_F - \epsilon_i^{\text{cl}}$ . Since

$$\text{Im} \ln \left[ \frac{i\epsilon_{\text{max}} + \Delta\epsilon}{iR + \Delta\epsilon} \right] = \text{Im} \ln \left[ \frac{\epsilon_{\text{max}}(1 - i\Delta\epsilon/\epsilon_{\text{max}})}{R(1 - i\Delta\epsilon/R)} \right] \quad (2.44)$$

$$= \text{Im} \ln(1 - i\Delta\epsilon/\epsilon_{\text{max}}) \quad (2.45)$$

as  $R \rightarrow \infty$ , (2.43) gives

$$F'_2 \approx \sum_i \frac{\partial \epsilon_i^{\text{cl}}}{\partial x} \left[ -\frac{1}{\pi} \frac{\epsilon_F - \epsilon_i^{\text{cl}}}{\epsilon_{\text{max}}} \right], \quad (2.46)$$

$$\approx 0 \quad (2.47)$$

for  $\epsilon_{\text{max}} \gg |\epsilon_F - \epsilon_i^{\text{cl}}|$ . Also, one can see in Fig. 1 that

$$\text{Im} \ln \left[ \frac{\epsilon_a - \epsilon_i^{\text{cl}}}{\epsilon_c - \epsilon_i^{\text{cl}}} \right] \rightarrow -\frac{1}{2}\pi \quad (2.48)$$

as  $R \rightarrow \infty$ , so

$$F_1 = -\frac{1}{2} \sum_i \frac{\partial \epsilon_i^{\text{cl}}}{\partial x}. \quad (2.49)$$

The expression for the electronic force thus simplifies to

$$F_x^{\text{el}} = -\frac{1}{2} \sum_i \frac{\partial \epsilon_i^{\text{cl}}}{\partial x} + F_2. \quad (2.50a)$$

However,  $V$  has no diagonal elements, so  $\sum_i \epsilon_i^{\text{cl}} = \text{Tr}H = \text{Tr}H_0 = \text{const}$ , and we have the further simplification  $F_1 = 0$ . This gives

$$F_x^{\text{el}} = F_2, \quad (2.50b)$$

where  $F_2$  is given by (2.42). Recall that the sample energies  $\epsilon_0^j$  of (2.42b) are distributed along  $C_2$  between  $\epsilon_F$  and  $\epsilon_F + i\epsilon_{\text{max}}$ , with nearly all the  $\epsilon_0^j$  near the real axis.

It is easy to see that (2.50) reduces to the result (2.23) for an isolated cluster if we neglect the energy dependence of  $H_{\text{sub}}$ , taking  $\epsilon_i(\epsilon) = \epsilon_i^{\text{cl}}$  and  $\psi_i(\epsilon) = \psi_i^{\text{cl}}$ . In this "cluster approximation," (2.42) becomes

$$F_2 = \frac{1}{\pi} \sum_i \frac{\partial \epsilon_i^{\text{cl}}}{\partial x} \text{Im} \ln \left[ \frac{\epsilon_F - \epsilon_i^{\text{cl}}}{\epsilon_a - \epsilon_i^{\text{cl}}} \right]. \quad (2.51)$$

First consider the occupied states with  $\epsilon_i^{\text{cl}} < \epsilon_F$ . Since  $\epsilon_a = \epsilon_F + iR$ , the quantity in parentheses equals  $(-i/R) |\epsilon_F - \epsilon_i^{\text{cl}}|$  in the limit  $R \rightarrow \infty$ . For the unoccupied states with  $\epsilon_i^{\text{cl}} > \epsilon_F$ , on the other hand, it is equal to  $(+i/R) |\epsilon_F - \epsilon_i^{\text{cl}}|$ . Choosing the branch of the logarithm such that  $\ln i = i\pi/2$  and  $\ln(-i) = -i\pi/2$ , we then obtain

$$F_2 = -\frac{1}{2} \sum_i \frac{\partial \epsilon_i^{\text{cl}}}{\partial x} \text{sgn}(\epsilon_F - \epsilon_i^{\text{cl}}) \quad (2.52)$$

and (2.50) becomes

$$F_x^{\text{el}} = -\sum_i \frac{\partial \epsilon_i^{\text{cl}}}{\partial x} \Theta(\epsilon_F - \epsilon_i^{\text{cl}}). \quad (2.53)$$

We mention that the summation over  $i$  in (2.53) and the previous equations includes a summation over spins, with spin degeneracy,  $\sum_i \rightarrow 2 \sum_r$ , where  $r$  labels a spatial state. We also mention two points in regard to the numerical calculations: First, one can minimize difficulties with the multivalued complex logarithm,  $\ln z$ , by using

$$\ln z = \ln r + i \tan^{-1}(y/x), \quad (2.54)$$

where  $r = (x^2 + y^2)^{1/2}$  and  $z = x + iy$ . One still has to stay on the proper branch of the multivalued inverse tangent function, of course, but this is not difficult: For  $\epsilon$  in the upper half plane,  $\text{Im} \epsilon_i(\epsilon)$  is always negative,<sup>3</sup> so  $y = \text{Im}[\epsilon_a^j - (\epsilon_i, \epsilon_0^j)]$  or  $\text{Im}[\epsilon_c^j - \epsilon_i(\epsilon_0^j)]$  is always positive in (2.42b). Also, we find in our calculations that  $x = \text{Re}[\epsilon_F - \epsilon_i(\epsilon)]$  ordinarily remains either positive or negative for a particular  $i$  as  $\epsilon$  decreases from  $\epsilon_F + i\epsilon_{\text{max}}$  to  $\epsilon_F$  along  $C_2$ . One is then always on the same branch, and the multivalued inverse tangent function can be replaced by its principal value. Even if  $x$  changes sign along  $C_2$ , one can choose the proper branch by monitoring the value of  $x$  as a function of  $\text{Im} \epsilon$ .

Since  $H_{\text{sub}}$  is non-Hermitian, one must calculate the eigenvectors of both  $H_{\text{sub}}$  and  $H_{\text{sub}}^\dagger$ —i.e.,  $\psi_i$  and  $\psi_i^\dagger$ —and then require the normalization

$$\bar{\psi}_i^\dagger \psi_i = 1. \quad (2.55)$$

As a check, we calculate  $\sum_i \psi_i \bar{\psi}_i^\dagger$  and find that it is very nearly equal to the identity matrix, so that completeness is satisfied.

At each time  $t$  during a simulation, one calculates the  $n \times n$  matrices  $H$  (Hamiltonian of isolated cluster),  $V = H - H_0$  (perturbation matrix),  $H_{\text{sub}}(\epsilon) = \epsilon - (G_0^{-1} - V)$  (subspace Hamiltonian for sample energies  $\epsilon = \epsilon_0^j$  along  $C_2$ ), and  $\partial V / \partial x$  (variation of interatomic matrix elements with atomic positions  $x$ ). Then the eigenvalue problem (2.30) is solved, and the electronic forces com-

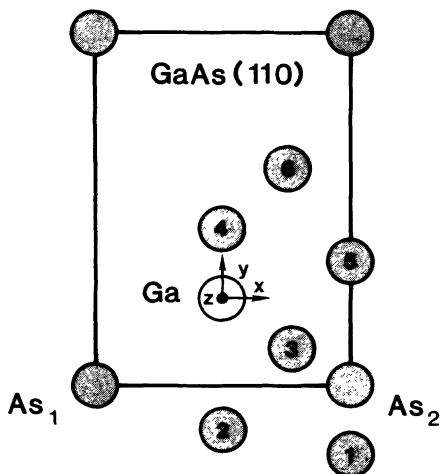


FIG. 2. Top view of (110) surface of GaAs, showing positions of Ga and As surface atoms and approximate positions of 6 initial chemisorption sites which have been observed in the present simulations.

puted from (2.31), (2.42), and (2.50). The computational bottle neck is solution of the two  $n \times n$  eigenvalue problems (2.30) for the non-Hermitian matrix  $H_{\text{sub}}$ , at each of the sample energies  $\epsilon_0^j$ , after each time step  $\Delta t$  of about  $10^{-15}$  sec. However, this calculation is rather fast with the computational resources now available; for example, with  $n = 36$ , a simulation of about 1000 time steps requires roughly an hour on a standard array processor.

### III. RESULTS

#### A. Preliminary discussion

The simulations of the present paper are for various chemical species impinging on the (110) surface of GaAs. Figure 2 shows a top view of this surface, with the choice of coordinates indicated. Our unit of length is half the GaAs bond length, or 1.225 Å. Then the As atoms at the lower and upper right corners, respectively, have coordinates (1.63, -1.15, 0) and (1.63, 3.45, 0) before they are allowed to relax. Figure 2 also schematically shows a top view of six possible chemisorption sites on the surface,

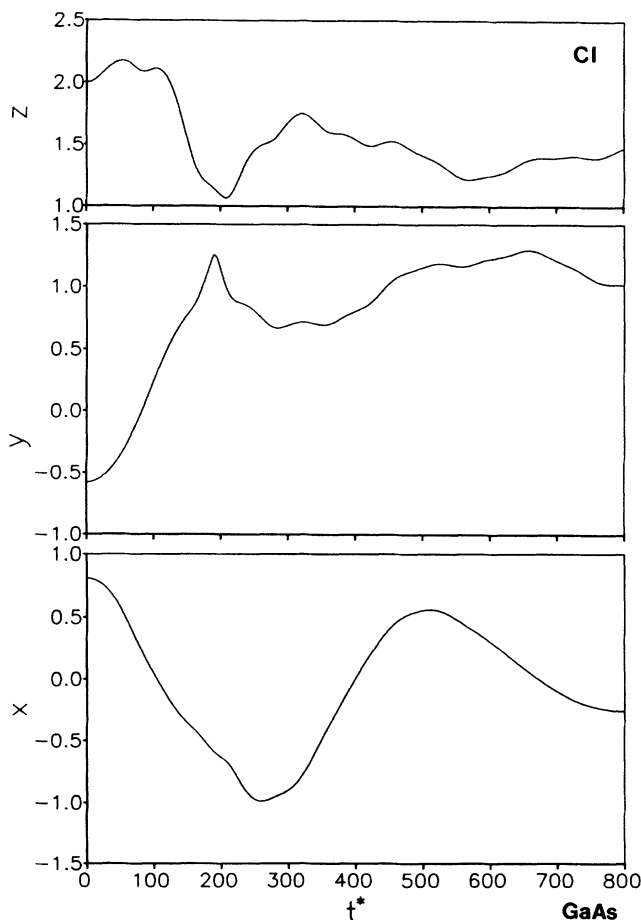


FIG. 3. Simulation of Cl chemisorbing on GaAs(110). The coordinate system is defined in Fig. 2. Distances are scaled by half the Ga—As bond length, 1.225 Å. The dimensionless time  $t^*$  is defined by  $t^* = t / \Delta t$ ,  $\Delta t = 1.04 \times 10^{-15}$  sec.

with bonding to a single As or Ga surface atom (1 or 4), to a pair of As or Ga atoms (2 or 5), or in a Ga—As bridge site (3 or 6). These positions, which are observed as initial chemisorption sites in our simulations of time-dependent chemisorption, have also been observed as energy minima along the surface in calculations of energy surfaces associated with static chemisorption.<sup>47,48</sup>

Let us begin by considering a test simulation in which there is no incoming atom, and the surface atom at the origin is placed at its unrelaxed position—i.e., the position it would have in bulk GaAs. We place the other atoms at fixed positions, so that only the atom at the origin is allowed to move. In four simulations—two with the surrounding atoms at their unrelaxed positions, and two with them at their relaxed positions—we found that the atom at the center relaxed in the way experimentally observed for GaAs(110). That is, As relaxes upward and Ga downward (with both atoms moving in the negative  $y$  direction), and by amounts that are in approximate agreement with the low-energy electron diffraction spectroscopy measurements.<sup>42,43</sup> These results—like those of Chadi,<sup>12,13</sup> Duke and co-workers,<sup>14</sup> and Sankey<sup>5</sup>—demonstrate that the present method yields the correct surface relaxation, an important initial requirement for any method that is to be applied in further studies of surface properties.

We choose the unit of time to be the same as the time step,  $\Delta t = 1.04 \times 10^{-15}$  sec, i.e.,  $t^* = t/\Delta t$ . In the simulations reported below, only two atoms are allowed to move—the surface atom at the origin and the incoming atom. The other atoms in the semi-infinite solid affect the simulation because they are electronically coupled to the moving atoms, as described in the preceding section, and they are also represented by repulsive potentials. They are, however, motionless in these first simulations with the present technique. As mentioned in the preceding section, the electronically perturbed subspace is larger than the movement subspace. With two atoms allowed to move, there are five atoms in the electronic subspace, since the surface Ga at the origin of Fig. 2 is bonded to three As neighbors. Since there are one  $s$  and three  $p$  orbitals per atom,  $H_{\text{sub}}$  and the other relevant matrices are  $20 \times 20$  in this case.

One could treat the propagation of vibrational energy into the solid with the time-dependent phonon Green's function.<sup>3,6,40</sup> In the present work, however, we simply reduce each velocity by 0.5% at each time step. This estimate of the appropriate rate of energy dissipation is based on our study of vibrational relaxation in a semi-infinite one-dimensional chain of atoms, with a sudden impulse applied at the end.<sup>6,40</sup>

Let us now turn to some representative simulations of various chemical species chemisorbing on GaAs(110). In each case, the surface atoms are initially motionless at their relaxed positions.<sup>42,43</sup> The initial position and velocity of the incoming atom can be read off the graphs. Recall that the unit of length is  $r_0/2$ , where  $r_0 = 2.45 \text{ \AA}$  is the bulk GaAs bond length.

Figure 3 shows a simulation for a Cl atom released with zero velocity and one GaAs bond length above the surface, at the Ga—As bridge site 3 of Fig. 2. This atom

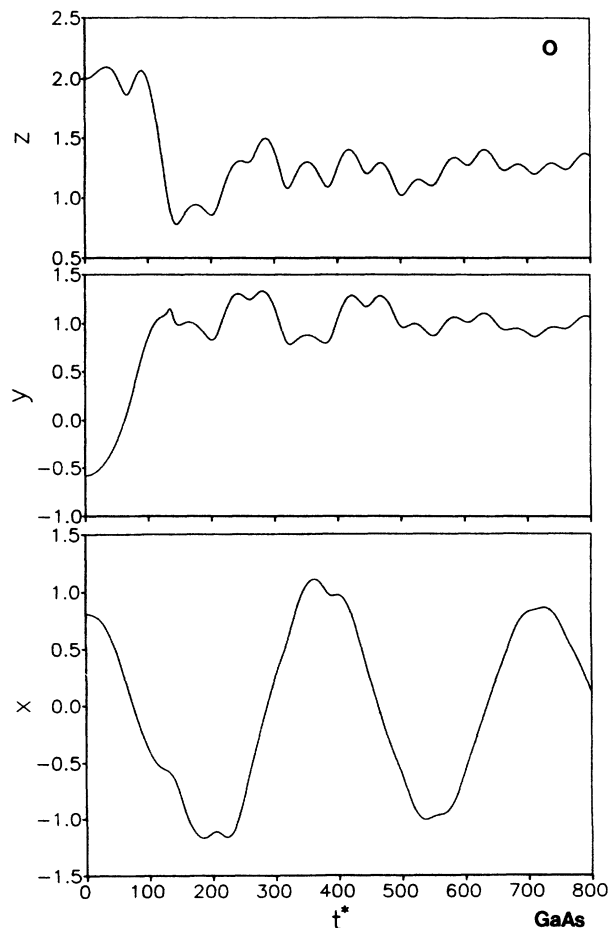


FIG. 4. O on GaAs(110).

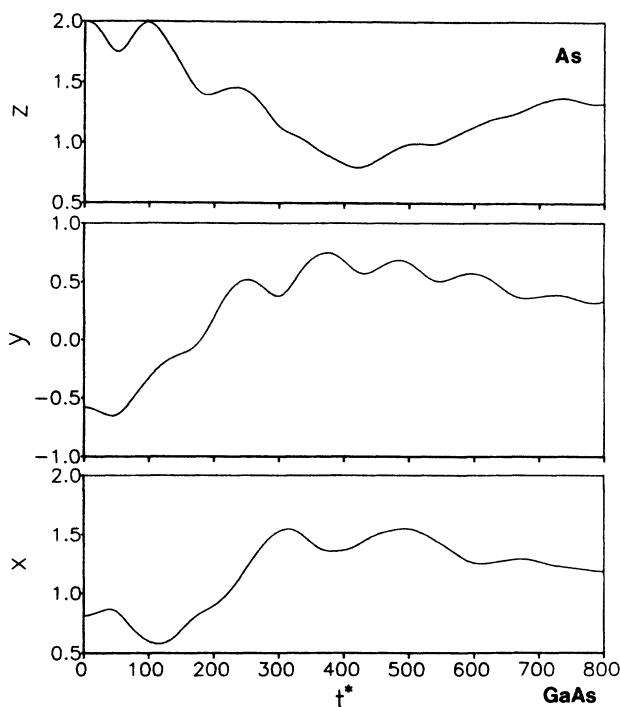


FIG. 5. As on GaAs(110).

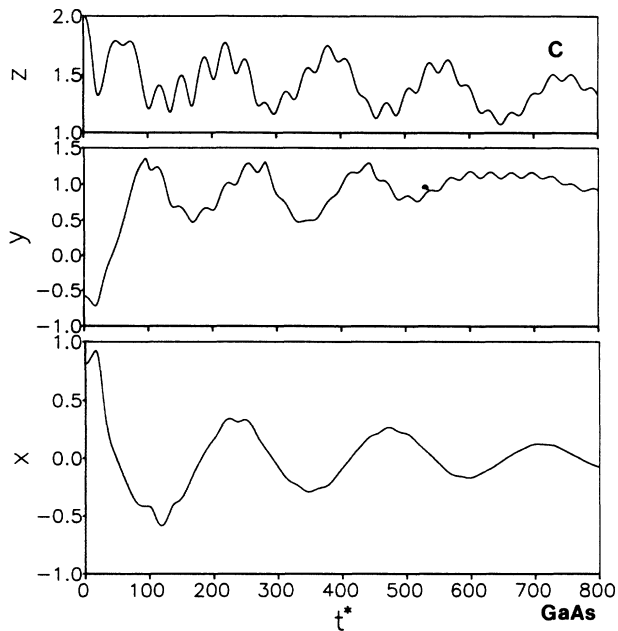


FIG. 6. C on GaAs(110).

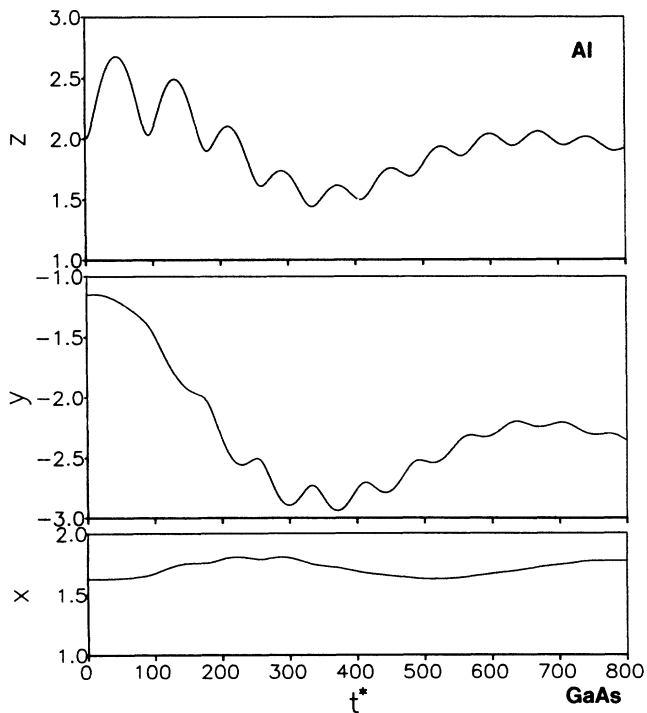


FIG. 8. Al on GaAs(110).

moves away from the surface As, and bonds to a single Ga at site 4 of Fig. 2. Since Cl is electronegative, this is just the kind of behavior one expects. Notice that the  $x$  vibrations of the Cl have large amplitude and a long period, because there is only a small, angle-bending restoring force for motion in that direction. We thus predict a low-frequency vibrational mode for this site. (Bonding to more distant neighbors will increase the fre-

quency of this mode somewhat, but it should still be relatively low.) Notice that the present technique automatically gives angle-bending as well as bond-stretching forces, with both resulting from changes in the total electronic energy as the atomic positions are varied. Also notice that one can study the equilibrium vibrations of surface and adsorbed atoms, even when such vibrations are highly anharmonic.

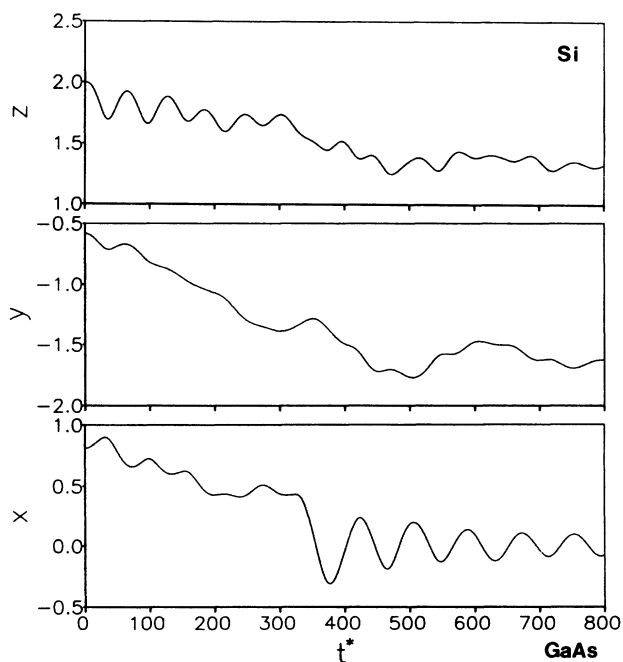


FIG. 7. Si on GaAs(110).

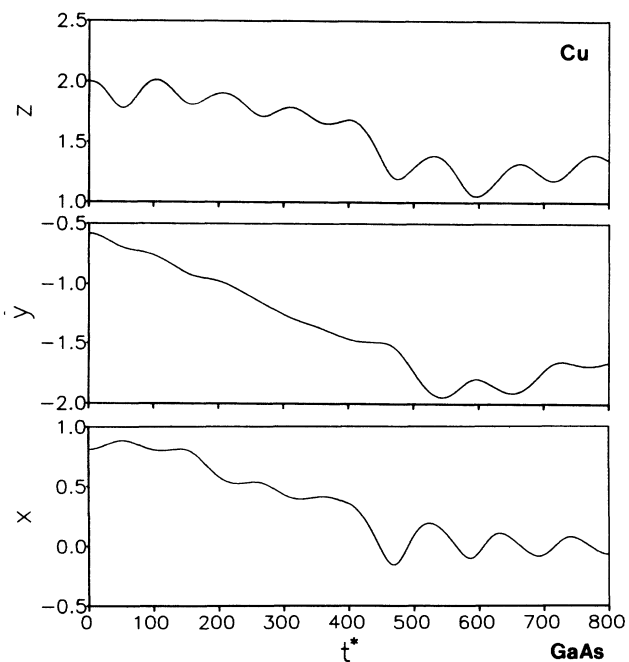


FIG. 9. Cu on GaAs(110).

Figure 4 shows a simulation for a 0 atom released with exactly the same initial conditions as the Cl shown above. Since O is light, it vibrates with high frequency in the y and z directions. Again, however, it vibrates with a long period and large amplitude in the x direction, for which there is only a small angle-bending restoring force (in a nearest-neighbor approximation). Figure 5 shows a simulation for As, which bonds at the Ga—Ga bridge site 5.

The initial conditions in the present simulations—zero velocity and the Ga—As bridge site 3—were chosen in order not to bias the motion of the chemisorbing atom. I.e., it can choose to bond either to the cation (Ga) or the anion (As). As one expects, the electronegative group-V, -VI, and -VII atoms tend to bond to the cation. Furthermore, it will be seen below that the electropositive group-I, -II, and -III atoms tend to bond to the anion. For group-IV elements, however, one expects that Ga and As will be about equally attractive. This is confirmed by the simulations of Figs. 6 and 7, which show C bonding to Ga, at site 4, but Si bonding at the As—As bridge site 2. Notice that the x vibrations of Si have higher frequency than those of C, even though Si is a heavier atom. The reason, of course, is that Si sits between two As atoms, above the surface, and experiences some bond-stretching restoring force. On the other hand, C is sub-

jected to only a weak angle-bending restoring force, like Cl and O in the simulations described above. The y and z motion of C show rapid vibrations, associated with bond stretching, superimposed on much slower vibrations, associated with angle bending. It is clear that the equilibrium vibrations of adsorbed atoms, like those of Figs. 6 and 7, provide a signature of the adsorption site.

In Fig. 8, an Al atom is released at a point exactly above a surface As. Initially repelled upward, apparently because of the outward As relaxation, the Al moves to site 1 of Fig. 2, where it bonds to the single As atom. Its high-frequency bond-stretching vibrations are superimposed on low-frequency vibrations, perpendicular to the As—Al bond, for this initial chemisorption site. Figure 9 shows a simulation for Cu. As one might expect, this electropositive atom is attracted by the anion, bonding at the As—As bridge site 2 for this set of initial conditions.

#### ACKNOWLEDGMENTS

We thank the U.S. Office of Naval Research for their support, which made this work possible, Grant No. N00014-82-K-0447. Additional support was provided by the Robert A. Welch Foundation (Houston, TX).

- <sup>1</sup>M. Menon and R. E. Allen, *Bull. Am. Phys. Soc.* **30**, 362 (1985).
- <sup>2</sup>M. Menon and R. E. Allen, in *Proceedings of the 1985 Summer Computer Simulation Conference, Chicago, 1985*, edited by the Society for Computer Simulation (North-Holland, Amsterdam, 1985).
- <sup>3</sup>R. E. Allen and M. Menon, *Phys. Rev. B* **33**, 5611 (1986).
- <sup>4</sup>M. Menon and R. E. Allen, *Phys. Rev. B* **33**, 7099 (1986).
- <sup>5</sup>O. F. Sankey and R. E. Allen, *Phys. Rev. B* **33**, 7164 (1986).
- <sup>6</sup>M. Menon and R. E. Allen, *Superlatt. Microstruct.* **3**, 295 (1987).
- <sup>7</sup>M. Menon and R. E. Allen, *Solid State Commun.* **64**, 353 (1987).
- <sup>8</sup>J. C. Slater and G. F. Koster, *Phys. Rev.* **94**, 1498 (1954).
- <sup>9</sup>D. J. Chadi and M. L. Cohen, *Phys. Status Solidi B* **68**, 405 (1975).
- <sup>10</sup>W. A. Harrison, *Electronic Structure and the Properties of Solids* (Freeman, San Francisco, 1980).
- <sup>11</sup>P. Vogl, H. P. Hjalmarson, and J. D. Dow, *J. Phys. Chem. Solid* **44**, 365 (1983).
- <sup>12</sup>D. J. Chadi, *Phys. Rev. Lett.* **41**, 1062 (1978); *Phys. Rev. B* **19**, 2074 (1979).
- <sup>13</sup>D. J. Chadi, *Phys. Rev. Lett.* **52**, 1911 (1984).
- <sup>14</sup>C. Mailhot, C. B. Duke, and D. J. Chadi, *Surf. Sci.* **149**, 366 (1985); Y. R. Wang, C. B. Duke, and C. Mailhot, *ibid.* **188**, L708 (1987); C. Mailhot, C. B. Duke, and D. J. Chadi, *Phys. Rev. B* **31**, 2213 (1985).
- <sup>15</sup>E. A. Kraut and W. A. Harrison, *J. Vac. Sci. Technol. B* **2**, 409 (1984); R. Enderlein and W. A. Harrison, *Phys. Rev. B* **30**, (1984).
- <sup>16</sup>A. Rahman, *Phys. Rev.* **136**, A405 (1964).
- <sup>17</sup>R. E. Allen, F. W. deWette, and A. Rahman, *Phys. Rev.* **179**, 887 (1969).
- <sup>18</sup>F. W. deWette, R. E. Allen, D. S. Hughes, and A. Rahman, *Phys. Lett.* **29A**, 548 (1969).
- <sup>19</sup>S. Shumway and R. E. Allen, *Surf. Sci.* **177**, L999 (1986).
- <sup>20</sup>F. H. Stillinger and A. Rahman, *J. Chem. Phys.* **60**, 1545 (1974).
- <sup>21</sup>F. H. Stillinger and T. A. Weber, *Phys. Rev. B* **31**, 5262 (1985).
- <sup>22</sup>M. Parrinello and A. Rahman, *Phys. Rev. Lett.* **45**, 1196 (1980).
- <sup>23</sup>M. Parrinello, A. Rahman, and P. Vashishta, *Phys. Rev. Lett.* **50**, 1073 (1983).
- <sup>24</sup>R. Car and M. Parrinello, *Phys. Rev. Lett.* **55**, 2471 (1985); *Solid State Commun.* **62**, 403 (1987).
- <sup>25</sup>H. C. Andersen, *J. Chem. Phys.* **72**, 2384 (1980).
- <sup>26</sup>J. C. Tully, *Surf. Sci.* **125**, 282 (1983).
- <sup>27</sup>F. F. Abraham, *J. Vac. Sci. Technol.* **2**, 534 (1984), and references therein.
- <sup>28</sup>U. Landman, R. N. Barnett, C. L. Cleveland, and R. H. Rast, *J. Vac. Sci. Technol. A* **3**, 1574 (1985), and references therein.
- <sup>29</sup>D. W. Brenner and B. J. Garrison, *Phys. Rev. B* **34**, 1304 (1986).
- <sup>30</sup>S. M. Paik, A. Kobayashi, S. Das Sarma, and K. E. Knor, in *The Physics of Semiconductors*, edited by O. Engström (World Scientific, Singapore, 1987), p. 1189.
- <sup>31</sup>M. Needels, M. C. Payne, and J. D. Joannopoulos, *Phys. Rev. Lett.* **58**, 1765 (1987).
- <sup>32</sup>N. Keating, *Phys. Rev.* **145**, 637 (1966).
- <sup>33</sup>E. Pearson, T. Takai, H. Halicioglu, and W. A. Tiller, *J. Cryst. Growth* **70**, 33 (1984).
- <sup>34</sup>R. Biswas and D. R. Hamann, *Phys. Rev. Lett.* **55**, 2001 (1985); *Phys. Rev. B* **34**, 895 (1986); in *The Physics of Semiconductors* edited by O. Engström (World Scientific, Singapore, 1987), p. 1173.
- <sup>35</sup>J. Tersoff, *Phys. Rev. Lett.* **56**, 632 (1986).
- <sup>36</sup>B. W. Dodson, *Phys. Rev. B* **33**, 7361 (1986); **35**, 2795 (1987).

- <sup>37</sup>K. Ding and H. C. Andersen, *Phys. Rev. B* **34**, 6987 (1986).
- <sup>38</sup>M. I. Baskes, *Phys. Rev. Lett.* **59**, 2666 (1987).
- <sup>39</sup>B. M. Deb, *Rev. Mod. Phys.* **45**, 22 (1973), and references therein.
- <sup>40</sup>M. Menon and C. W. Myles, *J. Phys. Chem. Solids* **48**, 621 (1987).
- <sup>41</sup>J. C. Tully, in *Many-Body Phenomena at Surfaces*, edited by D. Langreth and H. Suhl (Academic, London, 1984).
- <sup>42</sup>S. Y. Tong, A. R. Lubinsky, B. J. Mrstik, and M. A. van Hove, *Phys. Rev. B* **17**, 3303 (1978).
- <sup>43</sup>A. Kahn, E. So, P. Mark, and C. B. Duke, *J. Vac. Sci. Technol.* **15**, 580 (1978); C. B. Duke, R. J. Meyer, and P. Mark, *ibid.* **17**, 971 (1980).
- <sup>44</sup>A. Baldereschi, *Phys. Rev. B* **7**, 5212 (1973).
- <sup>45</sup>D. J. Chadi and M. L. Cohen, *Phys. Rev. B* **8**, 5747 (1973).
- <sup>46</sup>S. L. Cunningham, *Phys. Rev. B* **10**, 4988 (1974).
- <sup>47</sup>D. J. Chadi and R. Z. Bachrach, *J. Vac. Sci. Technol.* **16**, 1159 (1979).
- <sup>48</sup>J. Ihm and J. D. Joannopoulos, *Phys. Rev. B* **26**, 4429 (1982), and references therein.

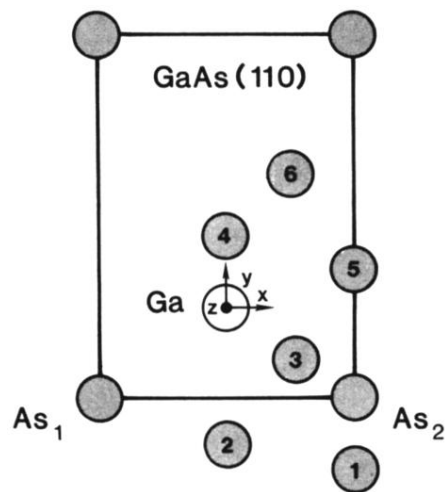


FIG. 2. Top view of (110) surface of GaAs, showing positions of Ga and As surface atoms and approximate positions of 6 initial chemisorption sites which have been observed in the present simulations.